

High Surface Area Silicon Carbide Whiskers and Nanotubes Nanocast Using Mesoporous Silica

Zhuxian Yang, Yongde Xia, and Robert Mokaya*

School of Chemistry, University of Nottingham, University Park, Nottingham NG7 2RD, U.K.

Received June 30, 2004. Revised Manuscript Received July 30, 2004

We report here the formation of high surface area silicon carbide materials comprising whiskers and nanotubes via a synthesis route, which utilizes mesoporous silica as sacrificial solid template. The silicon carbide materials are obtained via carbothermal reduction of mesoporous silica/carbon (i.e., SBA-15/sucrose) composites. Varying the carbothermal reduction conditions (i.e., temperature or duration) readily modifies the morphology of the silicon carbide so as to obtain whiskers or nanotubes. The whiskers, which grow in the [111] direction, are achieved by subjecting the mesoporous silica/carbon composites to carbothermal reduction at high temperature (1250 or 1300 °C) for reduction periods of up to 14 h. For reduction periods of up to 14 h, using the higher temperature (1300 °C) optimizes whisker formation. The diameter of the whiskers is 50–90 nm and their length is typically greater than 20 μm . The surface area of the whisker containing SiC materials varies between 120 and 145 m^2/g , while their pore volume is ca. 0.42 cm^3/g . Increasing the carbothermal reduction period to 20 h, at 1250 or 1300 °C, results in the formation of solid SiC nanotubes of diameter 60–100 nm and length greater than 10 μm . The formation of nanotubes is accompanied by an increase in the surface area (up to 190 m^2/g) of the silicon carbide materials.

Introduction

Silicon carbide (SiC) possesses unique properties such as high thermal conductivity, excellent thermal stability, mechanical strength, and chemical inertness.^{1–3} These properties make SiC a suitable material for various applications including the following: in semiconducting devices used at high temperature, high power, and high frequency,⁴ as the reinforcing phase in ceramics,⁵ or metal and polymer matrix composites,^{6,7} and as a catalyst support.^{1,8,9} Due to these unique properties and wide range of possible uses, much effort has been devoted to preparing SiC materials targeted at specific applications.^{10–15} For example, to be used as a catalyst support, it is desirable that (in addition to

the above-mentioned properties) the SiC possess medium to high surface area (20–100 m^2/g).¹⁶ For this reason there have been attempts to prepare high surface area SiC materials. Mesoporous SiC materials with surface area of 112¹⁷ and 120 m^2/g ¹³ have been prepared via a sol–gel method or chemical vapor infiltration (of pyrolytic carbon within the porosity of mesoporous silica MCM-48 in a temperature range 1250–1450 °C), respectively. Ledoux and co-workers prepared SiC with surface area ranging between 20 and 100 m^2/g using the so-called shape memory synthesis.^{1,8} The application of SiC as a catalyst support has been demonstrated for several reactions including, hydrodesulfurization,¹⁸ automotive exhaust-pipe reactions,⁹ isomerization of linear saturated hydrocarbons,¹ selective oxidation of hydrogen sulfide into elemental sulfur,¹⁹ and the selective oxidation of butane into maleic anhydride.²⁰ Surface area is thought to be an important consideration in the function of SiC as a catalyst support for these reactions. It is therefore desirable to investigate new synthesis methods to high surface area SiC.

The morphology of inorganic nanomaterials is known to have an important influence on their properties and use in various applications.¹⁴ For example, SiC whiskers

(1) Pham-Huu, C.; Bouchy, C.; Dintzer, T.; Ehret, G.; Estournes, C.; Ledoux, M. J. *Appl. Catal., A* **1999**, *180*, 385.

(2) Okada, K.; Kato, H.; Nakajima, K. *J. Am. Ceram. Soc.* **1994**, *77*, 1691.

(3) Bao, X.; Nangrejo, M. R.; Edirisinghe, M. J. *J. Mater. Sci.* **2000**, *35*, 4365.

(4) Feng, Z. C.; Mascarenhas, A. J.; Choyke, W. J.; Powell, J. A. *J. Appl. Phys.* **1988**, *64*, 3176.

(5) Becher, P. F.; Hsueh, C. H.; Angelini, P. T. *J. Am. Ceram. Soc.* **1988**, *71*, 1050.

(6) Chokshi, A. H.; Porter, J. R. *J. Am. Ceram. Soc.* **1985**, *68*, C144.

(7) Frevel, L. K.; Saha, C. K.; Petersen, D. R. *J. Mater. Sci.* **1995**, *30*, 3734.

(8) Pham-Huu, C.; Gallo, P. D.; Peschiera, E.; Ledoux, M. *J. Appl. Catal., A* **1995**, *132*, 77.

(9) Boutonet-Kizling, M.; Stenius, P.; Andersson, S.; Frestad, A. *Appl. Catal., B* **1992**, *1*, 149.

(10) Moene, R.; Makkee, M.; Moulijn, J. A. *Appl. Catal., A* **1998**, *167*, 321.

(11) Zhou, X. T.; Wang, N.; Lai, H. L.; Peng, H. Y.; Bello, I.; Wong, N. B.; Lee, C. S.; Lee, S. T. *Appl. Phys. Lett.* **1999**, *74*, 3942.

(12) Hu, J. Q.; Lu, Q. Y.; Tang, K. B.; Deng, B.; Jiang, R. R.; Qian, Y. T.; Yu, W. C.; Zhou, G. E.; Liu, X. M.; Wu, J. X. *J. Phys. Chem. B* **2000**, *104*, 5251.

(13) Parmentier, J.; Patarin, J.; Dentzer, J.; Vix-Guterl, C. *Ceram. Int.* **2002**, *28*, 1.

(14) Shen, G.; Chen, D.; Tang, K.; Qian, Y.; Zhang, S. *Chem. Phys. Lett.* **2003**, *375*, 177.

(15) Li, X. K.; Liu, L.; Zhang, Y. X.; Shen, S. D.; Ge, S.; Ling, L. *Ch. Carbon* **2001**, *39*, 159.

(16) Marchand, R.; Laurent, Y.; Guyader, J.; L'Haridon, P.; Verdier, P. *J. Eur. Ceram. Soc.* **1991**, *8*, 197.

(17) Jin, G.; Guo, X. *Microporous Mesoporous Mater.* **2003**, *60*, 207.

(18) Ledoux, M. J.; Hantzer, S.; Pham-Huu, C.; Guille, J.; Desaneaux, M. P. *J. Catal.* **1988**, *114*, 176.

(19) Keller, N.; Pham-Huu, C.; Crouzet, C.; Ledoux, M. J.; Savinponcet, S.; Nougayrede, J. B. *Catal. Today* **1999**, *54*, 535.

(20) Ledoux, M. J.; Crouzet, C.; Pham-Huu, C.; Turines, V.; Kourtakakis, K.; Mills, P. L.; Lerou, J. J. *J. Catal.* **2001**, *203*, 495.

are effective additives for reinforcement of various composite materials, mainly due to their high mechanical strength.⁵ The preparation of SiC whiskers is therefore important and has been achieved via various techniques, such as carbothermal reduction of silica^{21,22} or carbonaceous silica aerogels,¹⁵ decomposition of organic silicon compounds,²³ and reactions between silicon halides and carbon tetrachloride in the presence of hydrogen.²⁴ On a more general note, one-dimensional structured materials such as nanorods, nanowires, and nanotubes have recently attracted increasing interest due to their remarkable optical, electrical, and mechanical properties and their potential applications ranging from probe microscopy tips to interconnections in nanoelectrical devices.^{25,26} Tubular nanostructures have also been shown to be versatile catalyst supports in some reactions.²⁷ These findings have spurred an interest in tubular forms of SiC.^{11,12,14,28–31} Silicon carbide nanowires have been prepared by carbothermal reduction of silica²⁸ or sol–gel silica xerogels,^{29,30} and reduction–carburization of Si + CCl₄¹² or SiCl₄ + C₆Cl₆¹⁴ using sodium metal as reductant. SiC nanorods with diameters 2–20 nm have been obtained by reacting carbon nanotubes with Si and I₂ at 1200 °C.³¹ SiC nanorods have also been obtained from a solid carbon and silicon source on a Si substrate by hot filament chemical vapor deposition (HFCVD).¹¹ On the other hand, SiC nanotubes with medium surface area (30–60 m²/g) have been obtained by reaction between carbon nanotubes and silica vapor via the shape memory synthesis method.²⁷

Here, we report the synthesis and characterization of high surface area (120–190 m²/g) SiC whiskers and nanotubes obtained via carbothermal reduction of mesoporous silica/carbon (i.e., SBA-15/sucrose) composites. This study is motivated by the promising properties and possible uses expected from SiC materials that combine a well-defined nanotubular structure (whiskers or nanotubes) and high surface area. Our findings show that SiC whiskers are obtained at temperatures \geq 1200 °C and that higher temperatures favor the formation of whiskers. The formation of whiskers may also be optimized by increasing the time allowed for carbothermal reduction at any given temperature. Interestingly, extending the reduction period to 20 h at 1250 or 1300 °C results in the formation of SiC nanotubes.

Experimental Section

Material Synthesis. Mesoporous silica SBA-15 was prepared via established procedures.³² In brief, for the preparation

of SBA-15, a triblock polymer (Pluronic P123, EO₂₀PO₇₀EO₂₀, M_{av} = 5800, EO = ethylene oxide, PO = propylene oxide, Aldrich) was used as the structure-directing agent and tetraethoxysilicate (TEOS) as the silica source.³² The as-synthesized SBA-15 was calcined at 500 °C before being impregnated with sucrose via a two-step procedure similar to that normally used for the preparation of CMK-3 carbons.³³ The SBA-15/sucrose composite was then subjected to carbothermal reduction at 1200, 1250, or 1300 °C. The furnace temperature was raised to the final value at a heating ramp rate of 2 or 7.5 °C/min under argon flow and maintained at the target temperature for 7, 14, or 20 h. The resulting silica/carbon composites were washed with 10% hydrofluoric acid (HF) several times to remove the silica. This was followed by calcination of the HF-washed material at 700 °C for 2 h to eliminate any unreacted carbon. This calcination step was found to be extremely important in ensuring that the final material is purely SiC rather than a mixture of SiC and nanoporous carbon. The influence of preparation conditions (including reduction temperature and duration or heating ramp rate) on the SiC materials were investigated by varying the synthesis conditions. The samples were designated as SiC1200S, SiC1250S, and SiC1300S corresponding to carbothermal reduction temperature of 1200, 1250, and 1300 °C, respectively, with a slow heating rate of 2 °C/min and reduction duration of 7 h. Samples SiC1250MS and SiC1250MF correspond to materials reduced at 1250 °C for 14 h with a heating ramp rate of 2 and 7.5 °C/min, respectively. Samples SiC1250LF and SiC1300LF were reduced at 1250 and 1300 °C, respectively, for 20 h and a heating ramp rate of 7.5 °C/min.

Material Characterization. The SiC materials were characterized by powder X-ray diffraction (XRD), nitrogen sorption studies, thermogravimetric analysis (TGA), scanning electron microscopy (SEM), transmission electron microscopy (TEM), and X-ray photoelectron spectroscopy (XPS). Powder XRD analysis was performed using a Philips 1830 powder diffractometer with Cu K α radiation (40 kV, 40 mA). Nitrogen sorption isotherms and textural properties of the materials were determined at –196 °C using nitrogen in a conventional volumetric technique by a Coulter SA3100 sorptometer. Before analysis the samples were oven-dried at 150 °C and evacuated for 12 h at 200 °C under vacuum. The surface area was calculated using the BET method based on adsorption data in the partial pressure (P/P_0) range 0.05–0.2 and total pore volume was determined from the amount of the nitrogen adsorbed at P/P_0 = ca. 0.99. Thermogravimetric analysis (TGA) was performed using a Perkin-Elmer Pyris 6 TG analyzer with a heating rate of 20 °C/min in static air conditions. Scanning electron microscopy (SEM) images were recorded using a JEOL JSM-820 scanning electron microscope. Samples were mounted using a conductive carbon double-sided sticky tape. A thin (ca. 10 nm) coating of gold sputter was deposited onto the samples to reduce the effects of charging. Transmission electron microscopy (TEM) images were recorded on a JEOL 2000-FX electron microscope operating at 200 kV. Samples for analysis were prepared by spreading them on a holey carbon film supported on a grid. X-ray photoelectron spectroscopy (XPS) was performed using a Kratos AXIS ULTRA spectrometer with a monochromated Al K α X-ray source (1486.6 eV) operated at 10 mA emission current and 15 kV anode potential. The analysis chamber pressure was better than 10^{–9} Torr. FAT (fixed analyzer transmission) mode was used, with pass energies of 160 eV (or 80 eV) for survey scans and 40 eV for high-resolution scans. A magnetic immersion lens system allowed the area of analysis to be defined by apertures, a “slot” aperture of 300 \times 700 μ m for wide/survey scans and a 110 μ m aperture for high-resolution scans. The take-off angle for the photoelectron analyzer was 90° and the acceptance angle was 30° (in magnetic lens modes).

(21) Sharma, N. K.; Williams, W. S. *J. Am. Ceram. Soc.* **1984**, *67*, 115.

(22) Hollar W. E.; Kim, J. J. *Ceram. Eng. Sci. Proc.* **1991**, *12*, 979.

(23) Addamiano, A. J. *Cryst. Growth* **1982**, *58*, 617.

(24) Motojima, S.; Hasegawa, M. *J. Cryst. Growth* **1988**, *87*, 311.

(25) Alivisatos, A. P. *Science* **1996**, *271*, 933.

(26) Wong, E. W.; Sheehan, P. E.; Lieber, C. M. *Science* **1997**, *277*, 1971.

(27) Keller, N.; Pham-Huu, C.; Ehret, G.; Keller, V.; Ledoux, M. J. *Carbon* **2003**, *41*, 2131.

(28) Liu, J. W.; Zhong, D. Y.; Xie, F. Q.; Sun, M.; Wang, E. G.; Liu, W. X. *Chem. Phys. Lett.* **2001**, *348*, 357.

(29) Meng, G. W.; Cui, Z.; Zhang, L. D.; Philipp, F. J. *Cryst. Growth* **2000**, *209*, 801.

(30) Jin, G. Q.; Liang, P.; Guo, X. Y. *J. Mater. Sci. Lett.* **2003**, *22*, 767.

(31) Dai, H.; Wong, E. W.; Lu, Y. Z.; Fan, S. S.; Lieber, C. M. *Nature* **1995**, *375*, 769.

(32) Zhao, D.; Feng, J.; Huo, Q.; Melosh, N.; Fredrickson, G. H.; Chmelka, B. F.; Stucky, G. D. *Science* **1998**, *279*, 548.

(33) Jun, S.; Joo, S. H.; Ryoo, R.; Kruk, M.; Jaroniec, M.; Liu, Z.; Ohsuna, T.; Terasaki, O. *J. Am. Chem. Soc.* **2000**, *122*, 10712.

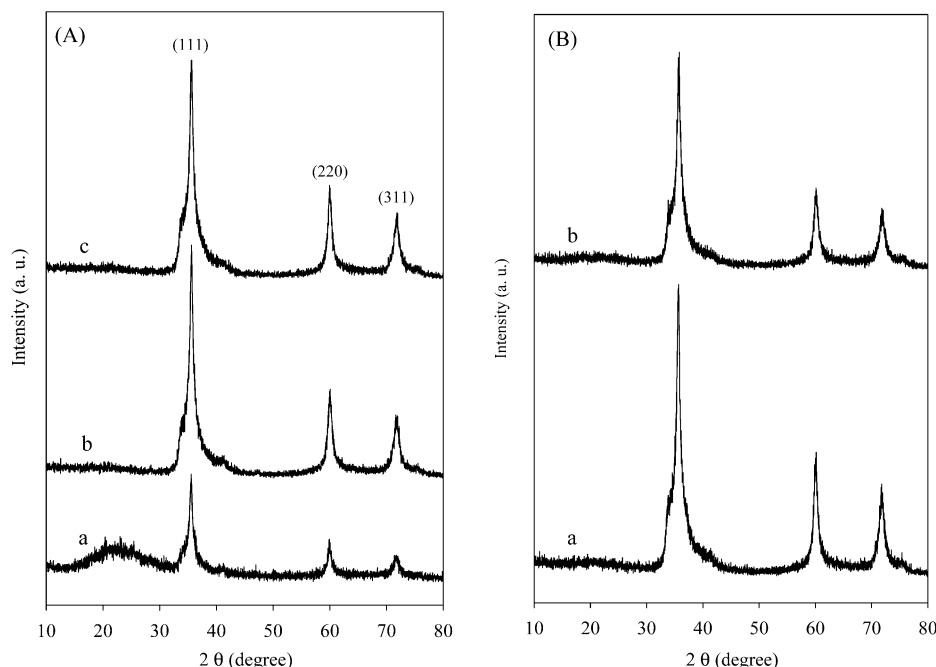


Figure 1. XRD patterns of SiC materials prepared at (A) a heating ramp rate of 2 °C/min and duration of 7 h at (a) 1200 °C (SiC1200S), (b) 1250 °C (SiC1250S), (c) 1300 °C (SiC1300S); and (B) a duration of 14 h at 1250 °C with a heating ramp rate of (a) 2 °C/min (SiC1250MS) and (b) 7.5 °C/min (SiC1250MF).

Results and Discussion

Textural Properties and Porosity. Figure 1 shows the powder X-ray diffraction (XRD) patterns of SiC prepared under various conditions. The XRD patterns indicate that the samples are all crystalline β -SiC. The XRD patterns show no evidence of other phases such as silica or carbon, implying that, if present, such impurities are either in trace amounts or are amorphous. (We note that the low 2θ angle regime of the XRD patterns was featureless.) The intensity of the diffraction peaks in Figure 1 indicates that the SiC materials have a highly crystalline structure. There is not much difference in the intensity of the XRD peaks for samples SiC1250S and SiC1300S (prepared at 1250 and 1300 °C, respectively), but the peak intensity for sample SiC1200S (prepared at 1200 °C) is much lower, implying a poorer crystalline character. The XRD pattern of sample SiC1200S also exhibits a broad peak centered at ca. 23° 2θ , which is due to residual silica. It can therefore be concluded that although SiC may be obtained via carbothermal reduction of silica/carbon composites at 1200 °C, the formation of β -SiC is favored at even higher (>1200 °C) temperatures. For this reason a temperature of 1250 °C was adopted for further investigations. We first note that no significant amounts of SiC were obtained at 1250 °C with a heating ramp rate of 2 °C/min and 7 h reduction duration. (This suggests that sufficient time has to be allowed for the carbothermal reduction to enable the conversion of the silica/carbon composite to SiC.) When the reduction duration increased to 14 h, SiC was obtained for both slow (2 °C/min) and fast (7.5 °C/min) heating rates (samples SiC1250MS and SiC1250MF, respectively) as shown by the diffraction peaks corresponding to β -SiC in Figure 1 (B). A comparison of the peak intensity of SiC1250MS and SiC1250MF indicates that, for extended reduction duration (i.e., 14 h), the heating rate has little effect on the formation of SiC.

Figure 2A shows the XRD patterns of SiC prepared at longer durations (14 or 20 h), with a heating rate of 7.5 °C/min at 1250 or 1300 °C (samples SiC1250MF, SiC1250LF, and SiC1300LF). There is little difference in the XRD patterns of the samples, indicating that, for longer reduction duration (≥ 14 h), a change of temperature from 1250 to 1300 °C does not significantly affect the overall crystallinity of the SiC formed. Figure 2B shows the nitrogen sorption isotherms corresponding to the XRD patterns in Figure 2A, i.e., SiC materials prepared at longer durations (14 or 20 h), with a heating rate of 7.5 °C/min at 1250 or 1300 °C (samples SiC1250MF, SiC1250LF, and SiC1300LF). All the materials exhibit adsorption at low partial pressure ($P/P_0 < 0.02$), which is due to micropore filling or capillary condensation. In addition to the uptake below $P/P_0 = 0.02$, the isotherms of the SiC materials exhibit adsorption at $P/P_0 > 0.1$, which may be attributed to the presence of mesopores from interparticle voids. For sample SiC1250MF (prepared at 1250 °C for 14 h), the adsorption (isotherm a) is mainly above $P/P_0 = 0.8$, thus suggesting a significant contribution from large mesopores perhaps arising from interparticle voids. The sorption isotherms of the other two samples, which were prepared for a longer carbothermal reduction period of 20 h, suggest the presence of a broad distribution of mesopores. It is possible that these samples possess framework-confined mesopores in addition to larger mesopores arising from interparticle voids. The isotherms in Figure 2B confirm that the SiC materials exhibit a significant level of porosity.

Table 1 shows the textural properties of SiC materials. The surface area of samples prepared for 7 or 14 h is in the range 120–145 m²/g, regardless of the heating ramp rate or carbothermal reduction temperature.¹³ For these samples, higher reduction temperature (sample SiC1300S) appears to favor high surface area, while a high heating ramp rate (sample SiC1250MF) results in

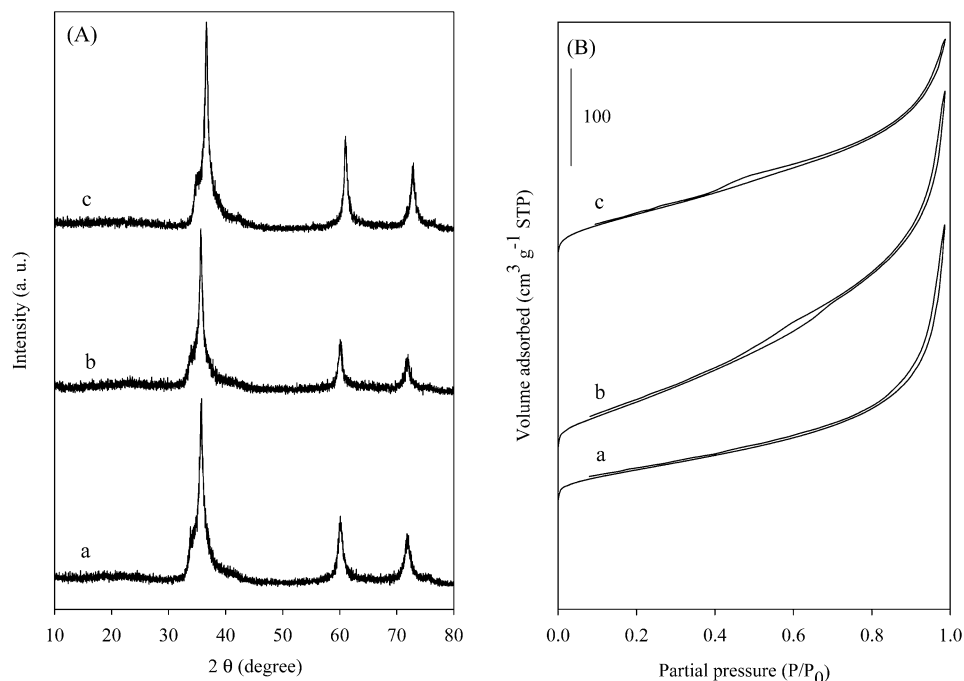


Figure 2. XRD patterns (A) and nitrogen sorption isotherms (B) of SiC prepared with a heating ramp rate of $7.5^\circ\text{C}/\text{min}$: (a) 1250°C , 14 h (SiC1250MF); (b) 1250°C , 20 h (SiC1250LF); (c) 1300°C , 20 h (SiC1300LF).

Table 1. Surface Area and Pore Volume of SiC Materials Prepared under Various Carbothermal Reduction Conditions

sample	temperature ($^\circ\text{C}$)	duration (h)	heating rate ($^\circ\text{C}/\text{min}$)	surface area (m^2/g)	pore volume (cm^3/g)
SiC1250S	1250	7	2	119	0.40
SiC1300S	1300	7	2	145	0.42
SiC1250MS	1250	14	2	140	0.43
SiC1250MF	1250	14	7.5	117	0.43
SiC1250LF	1250	20	7.5	181	0.55
SiC1300LF	1300	20	7.5	187	0.35

slightly lower surface area. The surface area of SiC materials prepared for longer duration (20 h) is much higher, i.e., 181 and $187 \text{ m}^2/\text{g}$ for samples prepared at 1250 and 1300°C , respectively. The reduction temperature does not appear to have any significant effect on the surface area of these 20 h samples. We note that the surface area observed for these samples is much higher than that of any previously reported SiC materials.^{13,17,27} The pore volume of all the SiC materials is also generally high (typically $0.4\text{--}0.55 \text{ cm}^3/\text{g}$). We believe that the high textural properties observed here are due to the use of ordered mesoporous silica (which possesses high surface area and pore volume) as the silica source. The mesoporous silica therefore also functions as a solid template.³³ The high surface area of the samples prepared at 1250 or 1300°C for 20 h (sample SiC1250LF and SiC1300LF) is consistent with the nitrogen sorption isotherms (Figure 2B), which suggest the presence of framework-confined mesopores. (It is worth noting here that the presence of significant amounts of residual carbon in the SiC materials results in a drastic increase in surface area and pore volume. For example, HF-washed SiC samples that were not subjected to the calcination step had a surface area of ca. $600 \text{ m}^2/\text{g}$ and a pore volume $>0.6 \text{ cm}^3/\text{g}$. The calcination step, which removes any residual carbon, is

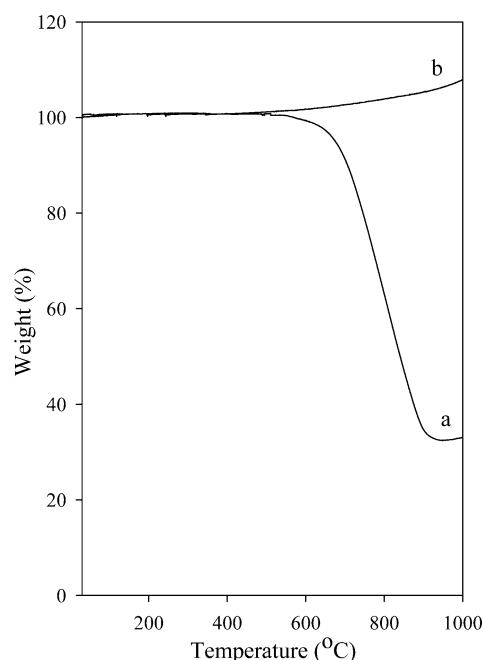


Figure 3. Thermogravimetric analysis curves of a representative SiC material (SiC1250LF) before (a) and after calcination at 700°C for 2 h.

therefore essential before any properties are ascribed to the SiC phase.)

The thermal stability of the SiC materials (in air) was assessed by thermogravimetric analysis (TGA). Since the materials were analyzed under static air conditions, the TGA was also useful in ascertaining the absence of residual carbon in the SiC materials. Figure 3 shows the TGA curves of SiC prepared at 1250°C for 20 h with a heating ramp rate of $7.5^\circ\text{C}/\text{min}$ (sample SiC1250LF) before and after calcination in air at 700°C . The weight loss that commences at ca. 600°C for the uncalcined sample is due to the combustion of unreacted carbon. No such weight loss is observed in the TGA curve of

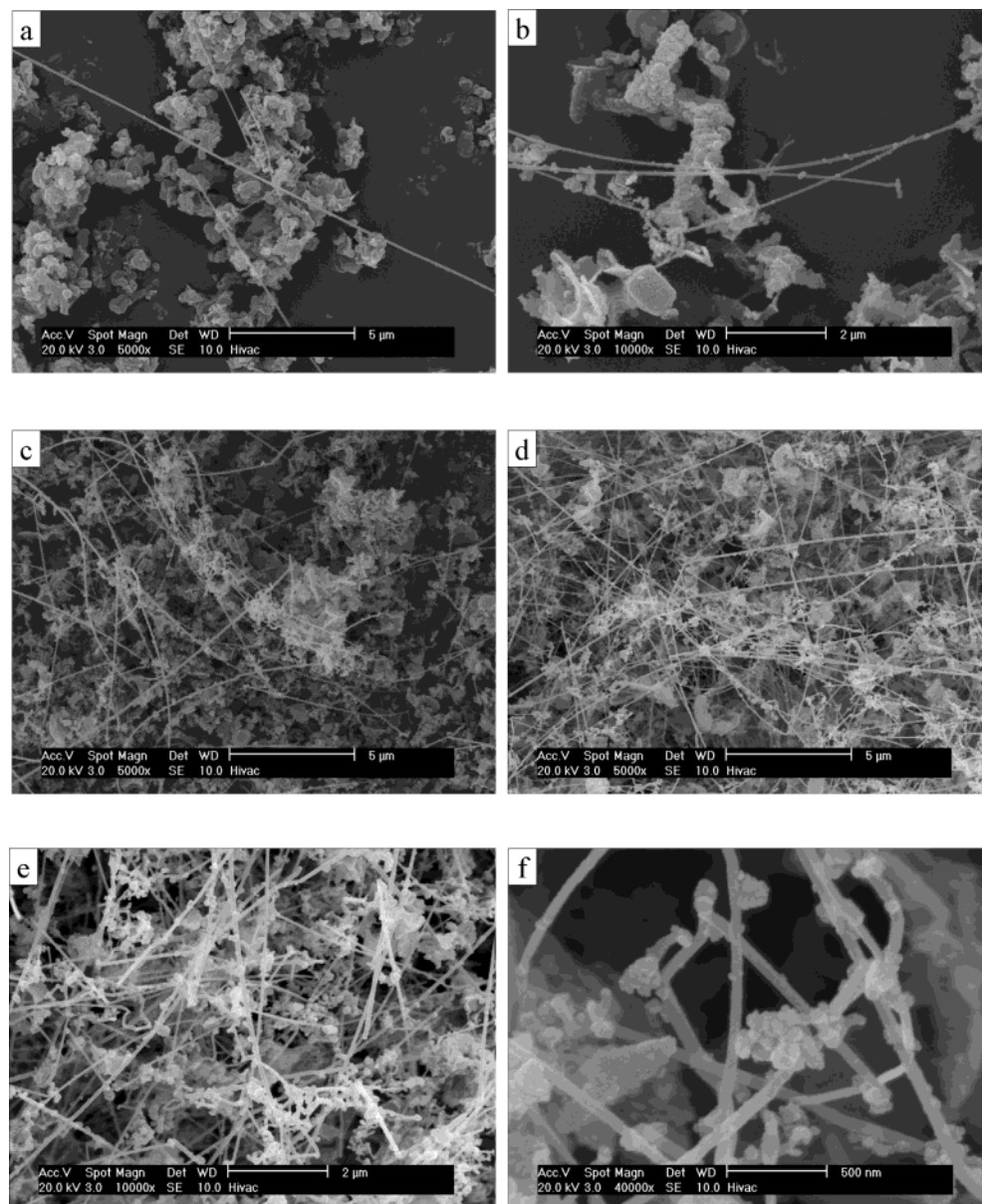


Figure 4. SEM images of SiC prepared with a heating ramp rate of 2 °C/min under various conditions (a) 1200 °C, 7 h (SiC1200S); (b) 1250 °C, 7 h (SiC1250S); (c) 1250 °C, 14 h (SiC1250MS); (d, e, f) 1300 °C, 7 h (SiC1300S).

the calcined sample (SiC1250LF). This indicates that any unreacted carbon in the HF-washed SiC samples is removed by calcination at 700 °C, which is the final step of the synthesis procedure. It is interesting to note that the weight of both samples starts increasing at ca. 900 °C, suggesting that SiC is oxidized under the prevailing oxidative (air) atmosphere, which is in agreement with previous reports.¹⁰

Morphology and Nanoscale Ordering. The particle morphology of the SiC materials was analyzed using SEM. Figures 4 and 5 show representative SEM images of a variety of SiC samples. Figure 4 shows images of samples prepared at various temperatures with a heating rate of 2 °C/min and duration of 7 or 14 h. Varying quantities of SiC whiskers of diameter 50–90 nm and length greater than 20 μm are present in all samples regardless of the reduction temperature. It is clear from the SEM images that the formation of SiC whiskers (as indicated by the proportion of particles that have whisker morphology) increases at higher temper-

ature or at longer reduction duration. Sample SiC1300S (prepared at 1300 °C) exhibited the highest proportion of whiskers, thereby confirming that, for durations of up to 14 h, higher temperatures favor the formation of SiC whiskers. Extending the carbothermal reduction duration to 20 h at either 1250 or 1300 °C had a remarkable effect on the particle morphology of the SiC; nanotubes were formed rather than whiskers. Figure 5 shows bundles of SiC nanotubes obtained for samples SiC1250LF and SiC1300LF. The SiC nanotubes, which have a diameter ranging from 60 to 100 nm and length typically greater than 10 μm , are solid tubes with smooth surfaces. The nanotubes observed here are therefore distinct from the hollow SiC nanotubes (with surface area around 30–60 m^2/g and rough surfaces) reported by Ledoux and co-workers.²⁷ The present SiC nanotubes are also distinguishable from previously reported nanorods³¹ and nanowires^{12,30} by their diameter and length. It is important to point out that the nanotubes were only observed for samples prepared for

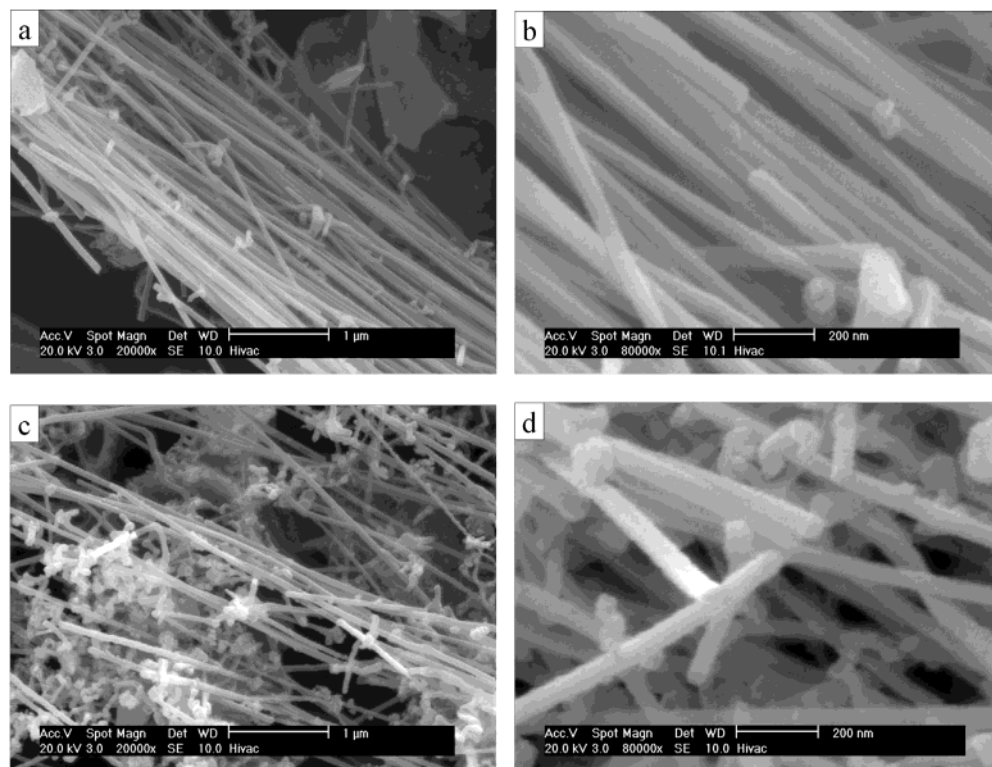


Figure 5. Representative SEM images of SiC nanotubes prepared at 1250 °C (SiC1250LF) (a,b) and 1300 °C (SiC1300LF) (c,d) with a heating ramp rate of 7.5 °C/min and carbothermal reduction duration of 20 h.

20 h. The formation of SiC solid-core nanotubes may be one reason for the extremely high surface area ($>180 \text{ m}^2/\text{g}$) observed for samples SiC1250LF and SiC1300LF. To the best of our knowledge, this is the first report on the preparation of SiC nanotubes that possess such a high surface area.

We investigated the local ordering of the SiC materials using TEM. Representative TEM images and selected area electron diffraction (SAED) patterns of SiC whiskers are shown in Figure 6. The morphology and nanoscale ordering depicted in Figure 6b–d is similar to that previously reported for known types of SiC whiskers.³⁴ On the other hand, the morphology in Figure 6a, which shows a whisker made of straight fiberlike bundles parallel to the [111] growth direction, is new and to the best of our knowledge has not been previously reported.^{34,35} The SAED pattern for this “straight fiber” containing whisker (inset Figure 6a) shows that it is highly crystalline. Figure 6b shows a whisker with a relatively flat surface and stacking-fault planes perpendicular to the [111] growth direction.^{34,35} Figure 6c shows a whisker with a rough sawtooth surface and stacking faults inclined to the growth direction while Figure 6d shows that some of the whiskers have a rough surface and stacking-fault planes inclined to the growth direction. The SAED pattern (inset Figure 6d) indicates a high degree of crystalline ordering. We observed no significant difference in the nanoscale ordering of whiskers prepared at 1250 and 1300 °C. This indicates that temperature (1250 or 1300

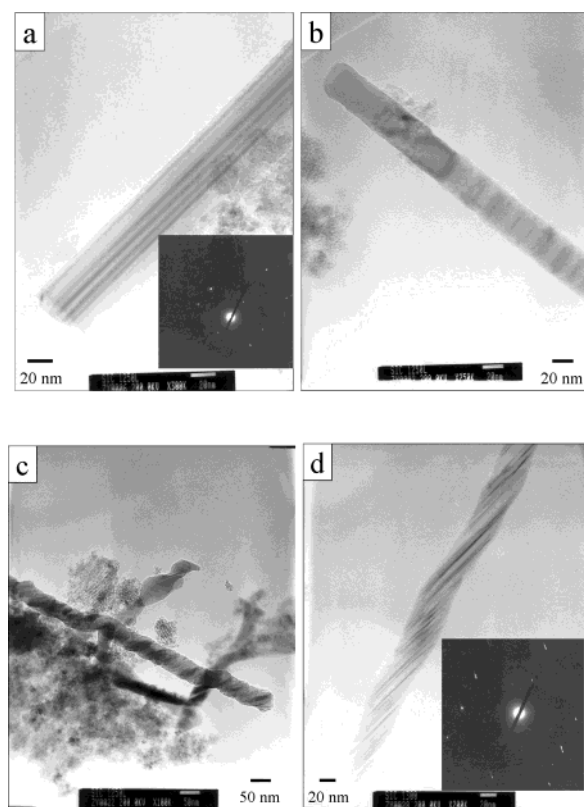


Figure 6. Representative TEM images of SiC materials prepared at a heating rate of 2 °C/min at 1250 °C (SiC1250MS) (a, b, c) for 14 h or 1300 °C (SiC1300S) (d) for 7 h. The insets in (a) and (d) are the corresponding SAED patterns.

°C) has little effect on the local ordering of the SiC whiskers and is consistent with the powder XRD patterns in Figure 1. It is interesting to note that Figure 6c indicates the presence of pore-channel type ordering

(34) Seo, W. S.; Koumoto, K.; Aria, S. *J. Am. Ceram. Soc.* **2000**, *83*, 2584.

(35) (a) Zheng, J.; Kramer, M. J.; Aknic, M. *J. Am. Ceram. Soc.* **2000**, *83*, 2961. (b) Wang, L.; Wada, H.; Allard, L. F. *J. Mater. Res.* **1992**, *7*, 148.

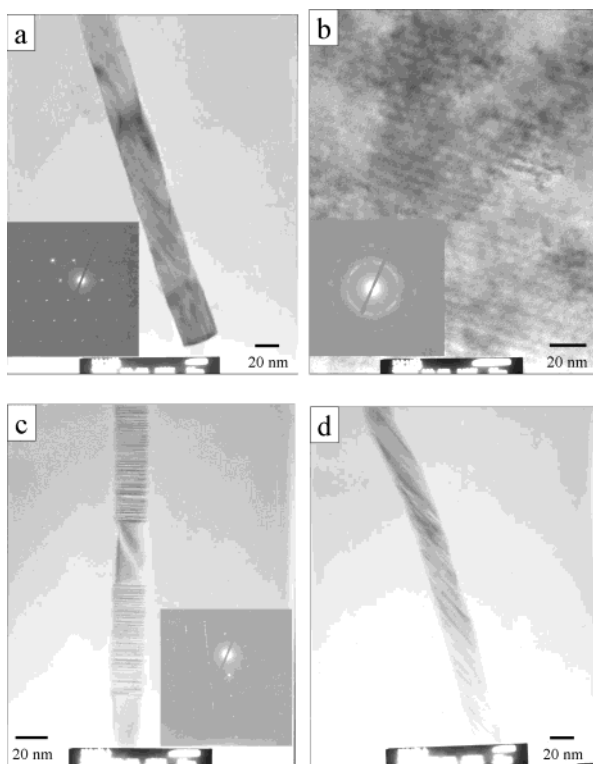


Figure 7. Representative TEM images of SiC materials prepared at a heating rate of 7.5 °C/min for a duration of 20 h at 1250 °C (SiC1250LF) (a, b, c) or 1300 °C (SiC1300LF) (d). The insets in (a), (b), and (c) are the corresponding SAED patterns.

for nonwhisker SiC particles. The pore channel type arrangement is clearly observed in the TEM image. The spacing calculated from the TEM image, i.e., ca. 5 nm, is consistent with the formation of the SiC via a mechanism where the mesoporous silica (SBA-15) acts as a solid template.³³ It is likely that the presence of such pore channel ordering contributes to the high surface area of the SiC materials.

Figure 7 shows representative TEM images of predominantly nanotubular SiC materials prepared for 20 h at 1250 or 1300 °C. Figure 7a shows a nanotube with a smooth surface and stacking faults inclined to the [111] growth direction. The corresponding SAED pattern confirms the crystalline nature of the nanotube. Figure 7b shows that the few non-nanotubular particles present in sample SiC1250LF possess some pore-channel type ordering (compare with Figure 6c). The corresponding SAED pattern of these particles shows that they are polycrystalline. The spacing calculated from the TEM image is ca. 5 nm, consistent with a nanocasting mechanism in which the SBA-15 mesoporous silica acts as a solid template.³³ Figure 7c shows a nanotube with stacking-fault planes perpendicular to the [111] growth direction. The SAED pattern (Figure 7c, inset) exhibits streaks in the diffraction pattern that are typical of a disordered layered structure.^{34,35} Figure 7d shows a nanotube with a smooth surface and stacking faults inclined to the [111] growth direction. The overall picture that emerges from the TEM studies is that the local ordering of the SiC whiskers and nanotubes is largely similar with respect to the nature of the stacking faults. However, the SAED patterns suggest that nanotubes, which are obtained from extended carbothermal reduction for 20 h, possess slightly higher levels of local ordering (crystallinity). This is consistent with the powder XRD patterns in Figure 2A.

Composition and Si–C Binding. Information on the binding between Si and C was obtained from XPS studies. Figure 8 shows the XPS spectra of representative SiC samples. The strong peak at 100.4 eV in Figure 8A corresponds to Si2p in SiC.³⁶ The other peak present in the spectra of sample SiC1200S at 103.3 eV corresponds to Si2p in SiO₂ and is due to residual silica. This confirms that, under our synthesis conditions, a temperature of 1200 °C is not sufficient for complete conversion of silica to SiC and is consistent with the XRD pattern in Figure 1A. The strong peak at 282.4 eV in Figure 8B corresponds to C1s in SiC, while the

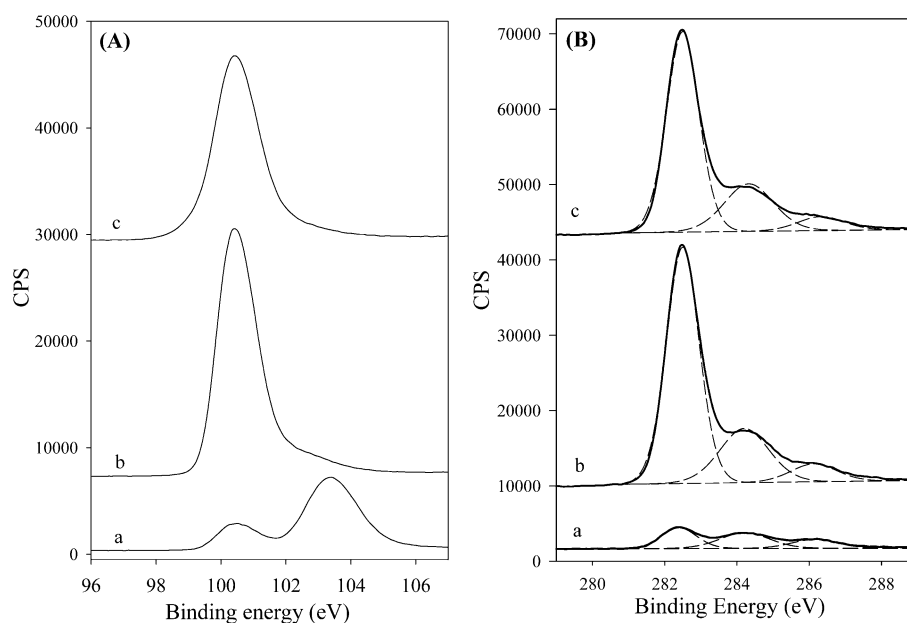


Figure 8. XPS spectra of Si 2p (A) and C 1s (B) for SiC materials prepared with a heating ramp rate of 2 °C/min for 7 h at (a) 1200 °C (SiC1200S), (b) 1250 °C (SiC1250S), and (c) 1300 °C (SiC1300S).

other two peaks at 284.2 and 286.2 eV correspond to residual or adventitious carbon on the surface of the SiC materials.³⁶ The XPS spectra therefore indicate that only trace amounts of residual carbon are present in SiC samples prepared at 1250 or 1300 °C, which is consistent with the XRD patterns in Figures 1 and 2A.

Conclusions

We have prepared high surface area (120–190 m²/g) SiC whiskers and nanotubes by carbothermal reduction of mesoporous silica/carbon (SBA-15/sucrose) composites at 1200–1300 °C under argon flow. SiC whiskers were obtained at a carbothermal reduction temperature of at least 1200 °C. Longer carbothermal reduction duration (up to 14 h) at 1250 or 1300 °C resulted in higher whisker production. The whiskers grew in the [111] direction with a diameter of 50–90 nm and their length

was typically greater than 20 μm. The surface area of the whisker containing SiC materials was between 120 and 145 m²/g, while their pore volume was ca. 0.42 cm³/g. High surface area (180–190 m²/g) solid core SiC nanotubes of diameter 60–100 nm, of length greater than 10 μm, and with smooth surfaces were obtained at 1250 or 1300 °C when the carbothermal reduction was performed for 20 h. The unique properties of the materials reported here (high surface area, whisker, or nanotubular morphology) combined with other well-known properties of SiC (i.e., high-thermal conductivity, high thermal stability, mechanical strength, and chemical inertness) provide new opportunities for the exploitation of SiC materials. Furthermore, the method presented here is facile and does not require catalysts or vacuum conditions to generate whiskers and nanotubes.

Acknowledgment. The authors are grateful to the EPSRC for financial support.

CM048950X

(36) Moulder, J. F. [et al.]; *Handbook of X-ray photoelectron spectroscopy: a reference book of standard spectra for identification and interpretation of XPS data*; Chastain, J., King, R. C., Ed.; Physical Electronics: Eden Prairie, MN, 1995.